

Enhancing the Performance of a Batch Electrocoagulation Reactor for Chromium Reduction Using Gas Sparging

M.A. Daous*, A.H. El-Shazly

Chemical and Materials Engineering Department, Faculty of Engineering, King Abdulaziz University, Jeddah, Saudi Arabia.

*E-mail: mdaous@kau.edu.sa

Received: 26 December 2011 / Accepted: 23 February 2012 / Published: 1 April 2012

This work investigates improving the performance of an electrocoagulation reactor for a hexavalent chromium reduction process by introducing gas sparging as a simple, cheap, and efficient method to improve the rate of mass transfer within the reactor. The effect of several variables on the reactor performance were investigated, such as the gas flow rate, initial Cr(VI) concentrations, the concentration of sodium chloride as an electrolyte solution, and the current density. Results show that, depending on current density employed, gas sparging can produce a 40 to 50 % improvement in Cr(VI) reduction and up to 90 % reduction in cell potential. Moreover, SEM and EDX analysis reveal that increasing gas flow rate leads to a decrease in the percentage of chromium adsorbed on the iron surface, which in turn decreases the possibility of anode surface passivation and enhances dissolution rate of iron anode and improves the unit performance.

Keywords: Electrocoagulation, hexavalent chromium, wastewater, gas sparging, electrochemical reactor

1. INTRODUCTION

Hexavalent chromium is well known for its toxicity. The element can potentially be released into aquatic environment by many different industries, such as those using Cr(VI) in organic synthesis or as an oxidizing agent, in metal finishing industries, chromate production, electroplating, tannery, fertilizer industries, and in industries employing Cr(VI) compounds as corrosion inhibitors, such as in cooling towers [1–3]. Reduction of Cr(VI) to Cr(III) by different reducing agents, such as NaHSO₃, FeS, FeSO₄, and SO₂, followed by chemical precipitation of Cr(III) by lime as Cr(OH)₃ has received a great attention [4-7]. Such method, however, suffer from the high cost of the chemicals used and their high required dosage. Typically, the chemical dosage required for Cr(VI) reduction is twice that

dictated by stoichiometry [7, 8]. More recently, electrochemical reduction methods using iron electrodes has received much attention owing to their operational simplicity, and the lesser amounts and cost of chemicals consumed in such a process than in direct chemical reduction methods [9, 10].

In such an electrolysis process, iron anodes dissolve in the electrolyte solution producing Fe^{2+} . Generated Fe^{2+} directly reduce present Cr(VI) to Cr(III) leading to the precipitation of $\text{Cr}(\text{OH})_3$ and $\text{Fe}(\text{OH})_3$. A sedimentation or flotation process is usually necessary to separate the sludge from the treated water. In such electrochemical process, no addition of chemicals is necessarily needed. Therefore, the maintenance and operation of the system is simple [11].

Previous investigations in the reduction of Cr(VI) to Cr(III) on iron ion surfaces in dilute solutions proved that the reduction reaction is diffusion controlled [12, 13]. It is therefore envisaged that the rate of reaction can be further increased by techniques that enhance the liquid-solid mass transfer by convection through induced solution circulation by mechanical agitation or gas sparging [14, 15, 16].

The aim of the present work is to investigate gas sparging as a mean to enhance the effectiveness of electrolytic removal of hexavalent-chromium from wastewater in a parallel plate electrochemical reactor. Gas sparging is widely used in many industrial applications employing gas-liquid contacting reactors. Typical examples can be found in oxidation, hydrogenation, and chlorination processes, wastewater treatments, and bioprocesses. Gas sparging columns or bubble columns have the advantages of being geometrically simple, free of moving parts and easy to manufacture. They provide superior gas-liquid interfacial mass and heat transfer, easy operation and cost effectiveness [14]. In 1975, Ibl et.al.[15] tested the effect of gas sparging on the rate of mass transfer in a parallel plate electrochemical reactor and concluded that gas sparging is an effective mean of liquid stirring that is cheaper than mechanical stirring. Gas sparging has been used since then to enhance the rate of liquid solid mass transfer at vertical plate electrodes [17], fixed bed electrodes [18], vertical fixed beds [19,20], and horizontal and vertical screens [21].

2. EXPERIMENTAL

2.1. Chemicals used

The following analytical grade reagents and chemicals were used in this study:

- Potassium dichromate ($\text{K}_2\text{Cr}_2\text{O}_7$) at different concentrations ranging from 0.01 to 0.02 M.
- Sulphuric acid and sodium hydroxide were used for solution pH adjustment.
- Sodium chloride (NaCl) solutions at different concentrations, ranging from 1.5 to 7.5 (w/w)%, were used for depassivation of iron electrodes, and increasing solution conductivity.
- Carbon tetrachloride was used for degreasing the electrodes.

2.2 Setup and procedure

The experimental setup and electrical circuit used in this study are shown in figure (1). The setup consisted of a 500 ml cylindrical glass cell of 7.5 cm diameter and 10 cm height, with a G4 type

sintered glass attached to its bottom to maintain a uniform gas flow into the cell. A 0.5 hp air compressor was used to supply needed air to the bottom of the cell through the sintered glass. Gas flow rate was measured by a rotameter and was controlled by a one way check valve that also prevented solution from flowing downward. Two monopolar iron electrodes were placed vertically inside the glass cell. These were consisting of a 2-cm diameter anode placed at the center of the cell with 4.5 cm of its height submerged in solution, and a hollow 0.1 cm thick iron cylinder lining the inner wall of the cell as a cathode. Before each experimental run, these electrodes were first immersed in a dilute carbon tetrachloride solution for few minutes to remove any residual grease or surface oxides, and washed with distilled water, and finally placed in their proper place in the cell and connected to a Potentiostat (AUTOLAB PGSTAT 30). In each run, 200 ml of acidified potassium dichromate solution at various initial concentration ranging from 0.01 to 0.02 M were first placed in the cell along with sodium chloride at different concentrations ranging from 1.5 wt.% to 7.5 wt.%. Air at different flow rate ranging from 2.5 to 10 liter/ min was sparged into the solution, while a constant current was applied to the cell for a total period of 30 minutes. A current density ranging from 3.0 to 10 mA/cm² was employed in these experiments. Cr(VI) concentration at the end of each experiment was determined by titrating a measured solution sample with a standard 0.1 N ferrous ammonium sulphate using diphenylamine barium salt as an indicator [22]. The percentage of Cr(VI) removed at the end of each experiment was then calculated as follows

$$\% \text{ Cr(VI) removed} = 100(C_0 - C)/C_0$$

Where C_0 is the initial Cr(VI) concentration and C is the Cr(VI) concentration at the end of electrolysis procedure. Cell and electrode potentials, and cell power consumption was monitored in each experiment to allow for evaluating cell performance and its economic viability at the different investigated operating conditions.

2.3 Scanning electronic microscope (SEM) and energy dispersive analysis EDX

Anodes subjected to tests conducted at different gas flow rates and different initial dichromate concentrations were further studied by SEM (JSM-6360LA, JEOL, Tokyo, Japan, using 20 kV accelerating voltage), and an energy dispersive analysis, EDX, (EX-23000BU attached unit).

3. RESULTS AND DISCUSSION

The main reactions taking place in the electrochemical cell are as follows [9, 10]:
Anodic dissolution of iron takes place at the iron anode according to the reactions



The resulting Fe^{2+} ions are oxidized to Fe^{3+} by Cr^{6+} according to the reaction



At the cathode two simultaneous reactions take place, namely



The anodically formed Fe^{3+} combines with the cathodically formed OH^- to produce insoluble $\text{Fe}(\text{OH})_3$

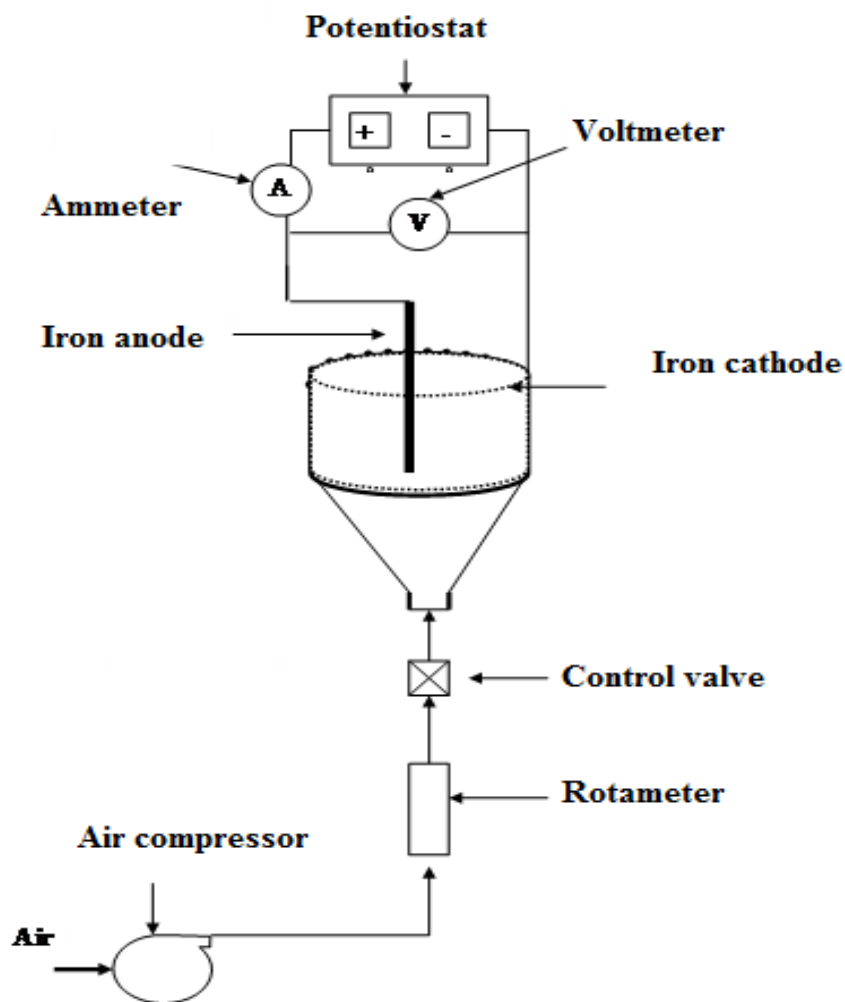


Figure 1. experimental setup

It is also possible that some of the anodically formed Fe^{2+} ions are oxidized to $\text{Fe}(\text{OH})_3$ by the sparged air. Since $\text{Fe}(\text{OH})_3$ is known to be a strong adsorbent [10], it adsorbs $\text{Cr}(\text{VI})$ as well as $\text{Cr}(\text{III})$ ions. Thus in such a gas sparged electrochemical reactor cell, hexavalent chromium is removed via (i) cathodic reduction (ii) reduction by the anodically formed Fe^{2+} and (iii) electrocoagulation where $\text{Cr}(\text{VI})$ and $\text{Cr}(\text{III})$ are adsorbed on $\text{Fe}(\text{OH})_3$ followed by air bubble flotation to the solution surface.

3.1. Effect of gas flow rate and current density on $\text{Cr}(\text{VI})$ removal

Figure 2 shows the effect of current density on the percentage removal of $\text{Cr}(\text{VI})$ at different air superficial velocities. Data of figure 2 reveal that removal of $\text{Cr}(\text{VI})$ increases with increasing current density and air velocity, which is consistent with Faraday's law according to which the rate of cathodic reduction of $\text{Cr}(\text{VI})$ as well as the rate of reduction by the anodically formed Fe^{2+} should increase with increasing current density.

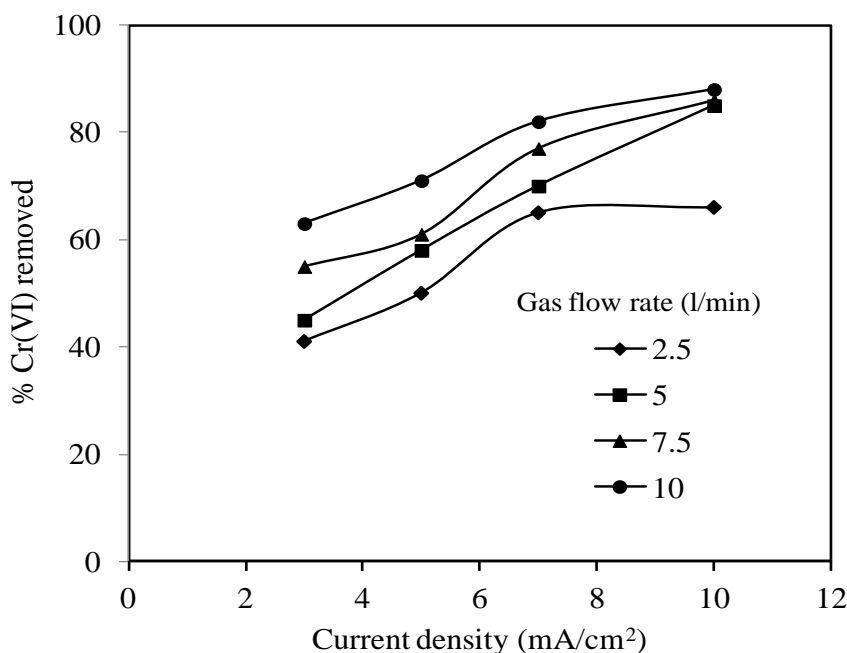


Figure 2. % $\text{Cr}(\text{VI})$ removed vs. current density at different gas flow rate. Initial potassium dichromate solution concentration = 0.01 M, and NaCl concentration = 3.5 wt. %

The increase in $\text{Cr}(\text{VI})$ removal with increasing air superficial velocity is attributed to the fact that rising gas bubbles improve the mixing efficiency in the solution bulk by virtue of their ability to introduce micro and macro convection in the axial and radial direction [18]. The resulting good mixing conditions enhance the aforementioned reactions, thus leading to a faster $\text{Cr}(\text{VI})$ removal. Moreover, turbulence generated by the rising gas bubbles enhances the rate of mass transfer at the anode and cathode with a consequent decrease in concentration polarization which tends to slow down the rate of cathodic and anodic reactions and may lead to anode passivation especially at high current densities.

However it is observed that the beneficial effect of increasing air velocity diminishes at higher velocities; probably because vigorous stirring resulting at high air flow rate re-disperses the coagulated $\text{Fe}(\text{OH})_3$ with its adsorbed $\text{Cr}(\text{VI})$, $\text{Cr}(\text{III})$ ions. A similar effect was observed by other investigators who tested the effect of mechanical stirring on the rate of electrocoagulation [23]. The effect of gas sparging on the anodic potential at different gas flow rates is shown in figure 3. Results show that, depending on gas flow rate used, up to 90% reduction in the anodic potential can be achieved, which indicates that gas sparging can decrease the anodic over potential to a good extent, which in turn improves the electrochemical reactor performance.

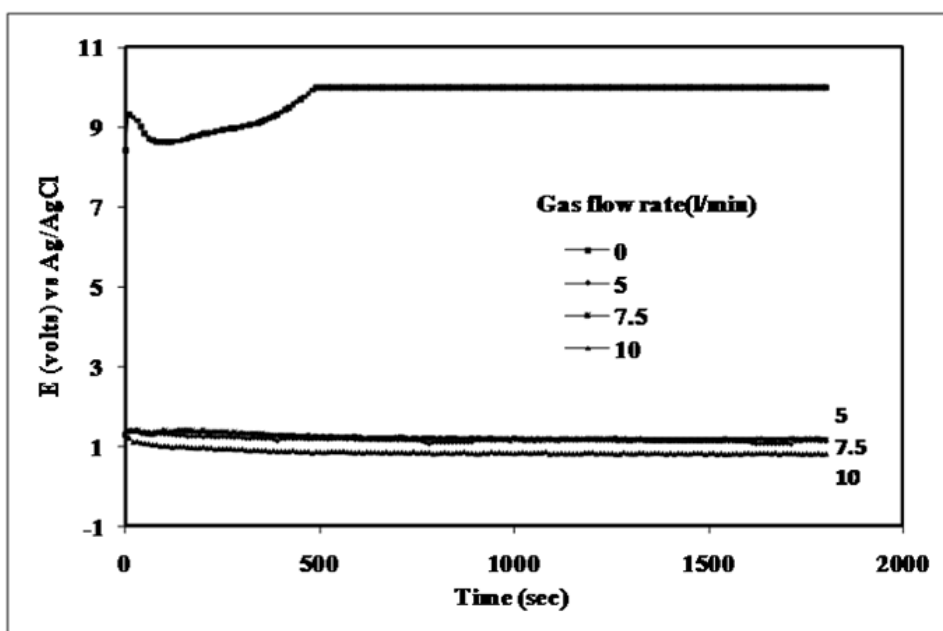


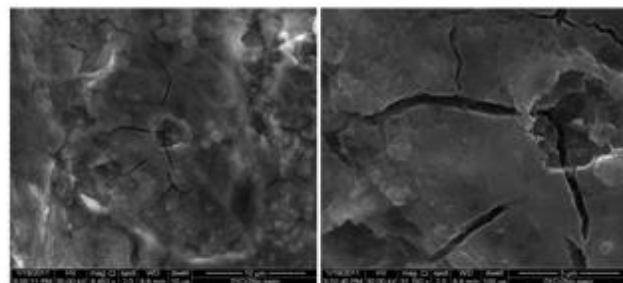
Figure 3. Change of anodic potential with time at different gas flow rate. Initial potassium dichromate solution concentration = 0.01 M, and NaCl concentration = 3.5 wt. %

3.1.1. Effect of gas sparging on the anode surface morphology and composition

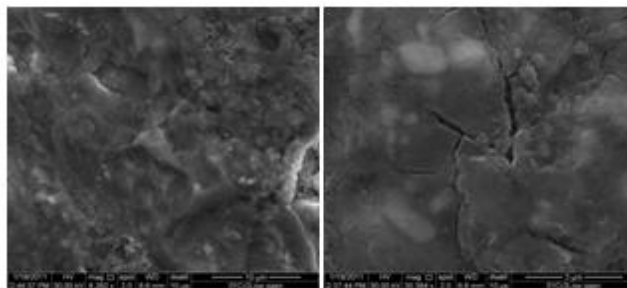
Scanning electronic microscopy (SEM) and energy dispersive analysis (EDX) were used to investigate the effect of gas sparging on the anodic surface morphology and composition respectively. Results of these investigations are illustrated in figure 4 and table 1. These results clearly reveal that increasing gas flow rate tends to decrease the percentage of chromium adsorbed on the anode iron surface. This in turn decreases the possibility of surface passivation and enhances the rate of dissolution of iron anode, which leads to improving the unit performance. Figure 4a clearly reveals that, when no gas sparging is used, a clear deposited layer of chromium develops on the anode surface. Figure 4c, on the other hand, shows that at higher gas flow rates (10 l/min), the anode surface is almost clear of adsorbed layers and that the dissolution of anode takes place at different points of the surface. These findings clearly show that gas sparging can substantially enhance the unit performance by both improving the mass transfer in the unit and by preventing anode surface passivation.

Table 1. Anode surface composition after subjected to different gas flow rate at 0.01 M initial concentration of potassium dichromate solution and 1.5 wt.% NaCl solution.

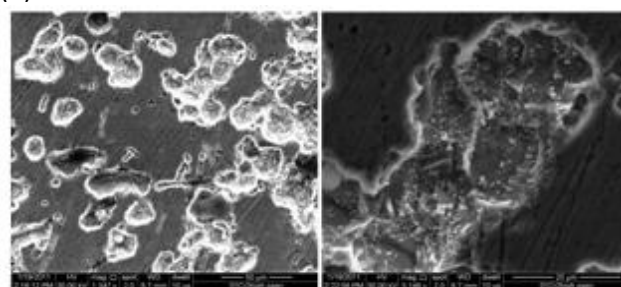
Surface location	No gas flow		Gas flow rate=5 l/min		Gas flow rate=10 l/min	
	%Cr	%Fe	%Cr	%Fe	%Cr	%Fe
Overall	2.63	97.37	1.68	98.32	1.48	98.52
001	6.96	93.04	3.91	96.09	0.35	99.65
003	1.01	98.99	0.62	99.38	0.26	99.74



(a)



(b)



(c)

Figure 4. SEM images of anode surface at different gas flow rate (a) no gas flow, (b) gas flow rate = 5 l/min, and (c) gas flow rate= 10 l/min.

3.2. Effect of sodium chloride concentration

Figure 5 shows the effect of the NaCl electrolyte solution concentration on the removal of Cr(VI). Results shown in figure 5 reveal that at relatively low NaCl concentrations, removal of Cr(VI)

increases with increasing NaCl concentration. This increase, however, diminishes beyond a certain NaCl concentration.

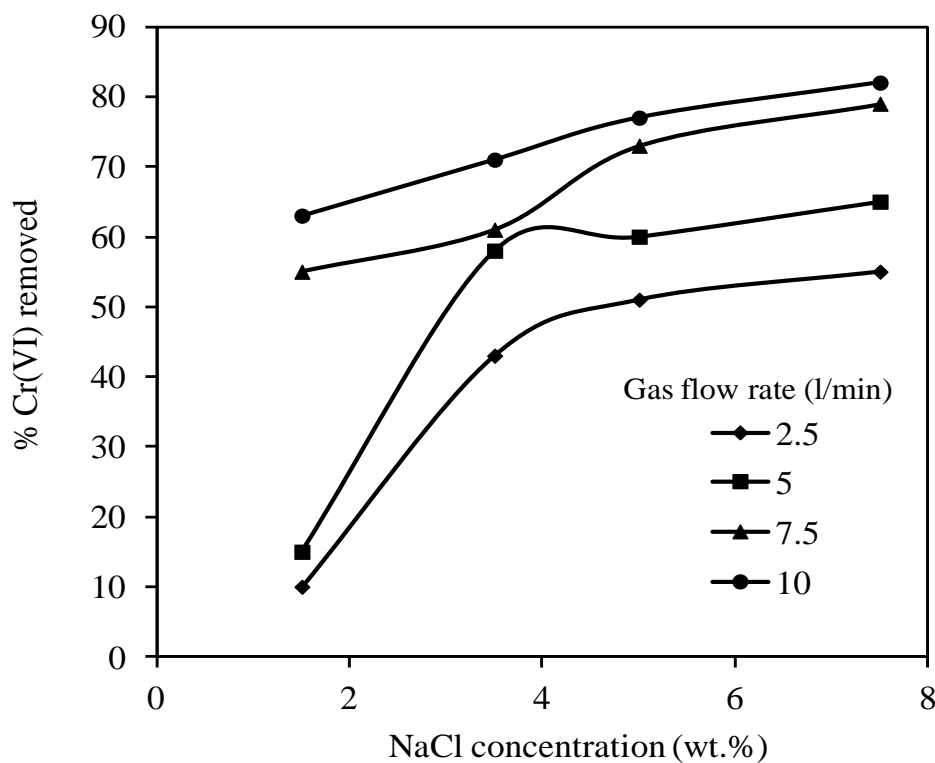


Figure 5. % Cr(VI) removed vs. NaCl concentration at different gas flow rates, current density = 5 mA/cm², and initial potassium dichromate solution concentration = 0.02M.

The beneficial effect of an initial increase of NaCl concentration on the Cr(VI) removal can be attributed to the role of Cl⁻ ions in overcoming anode passivation that may take place at high current densities by virtue of the ability of Cl⁻ to destroy the iron oxide film formed on the anode. A passive Fe anode would evolve oxygen instead of producing Fe²⁺ ions. On the other hand, the diminishing effect of NaCl concentration at higher concentrations may be explained by (i) a further increase in NaCl concentration results in an increase in the interionic attraction between Cl⁻ and Fe²⁺. This would reduce the diffusivity of Fe²⁺ ions with a consequent decrease in their transfer from the anode surface to the solution bulk.

This in turn would increase ionic polarization and slow down anodic dissolution. This explanation is further supported by the data of figure 6, which shows that the anodic potential does increase by increasing NaCl concentration above 3.5%. (ii) Higher NaCl concentrations tend to increase the solubility of Fe(OH)₃, which absorbs Cr(VI) and Cr(III) ions.

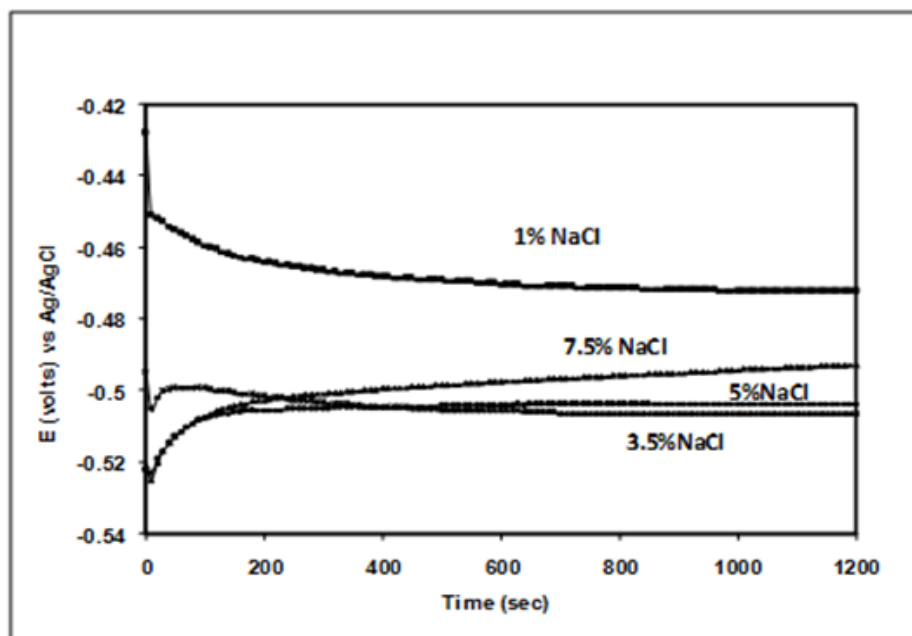


Figure 6. Change of cell potential with time at different NaCl concentrations, current density = 5 mA/cm², and initial potassium dichromate solution concentration = 0.02M.

3.3. Effect of initial Cr(VI) concentration

Figure 7 shows that the percent of Cr(VI) removed decreases with increasing the initial chromate concentration.

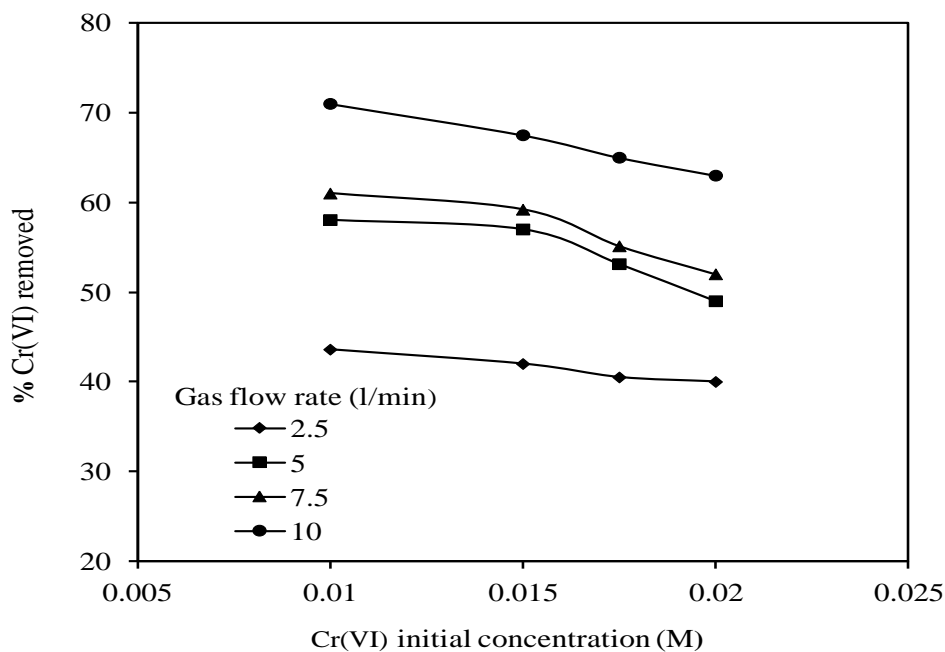


Figure 7. % Cr(VI) removed vs. initial potassium dichromate solution concentration at different gas flow rates, current density = 10 mA/cm², and NaCl concentration = 1.5 wt.%.

This is due to two factors: (i) under the present experimental conditions, available $\text{Fe}(\text{OH})_3$ coagulant is limited and their active surface area can become fully saturated with $\text{Cr}(\text{VI})$ and $\text{Cr}(\text{III})$ ions with no more active surface left to adsorb further chromium ions. (ii) It is also possible that higher $\text{Cr}(\text{VI})$ concentration tends to passivate the anode chemically. SEM and EDX analysis were used to verify this point. Figure 8 shows a sample SEM image and table 2 presents such EDX data, which reveal that increasing the initial $\text{Cr}(\text{VI})$ concentration lead to an increase in the concentration of chromium adsorbed on the anode iron surface. This is also reflected in the SEM image of figure 9, which shows a thicker deposited layer of chromium formed on the anode surface when using higher initial chromate solution concentration.

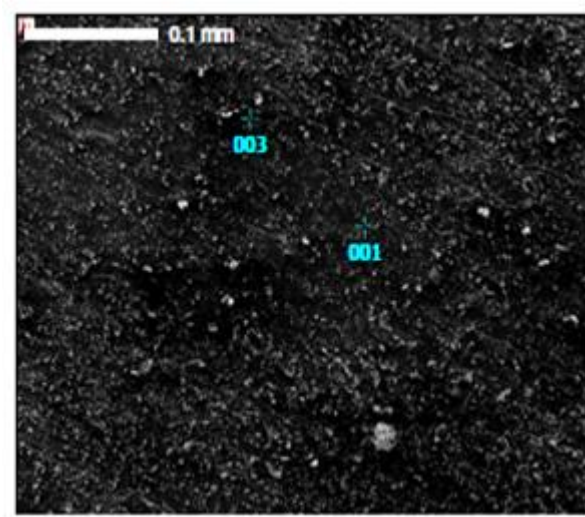


Figure 8. A sample of SEM image of anode surface at no gas flow rate, 0.01 M initial concentration of potassium dichromate solution, 5 mA/cm^2 current density, and 1.5 wt. % NaCl solution.

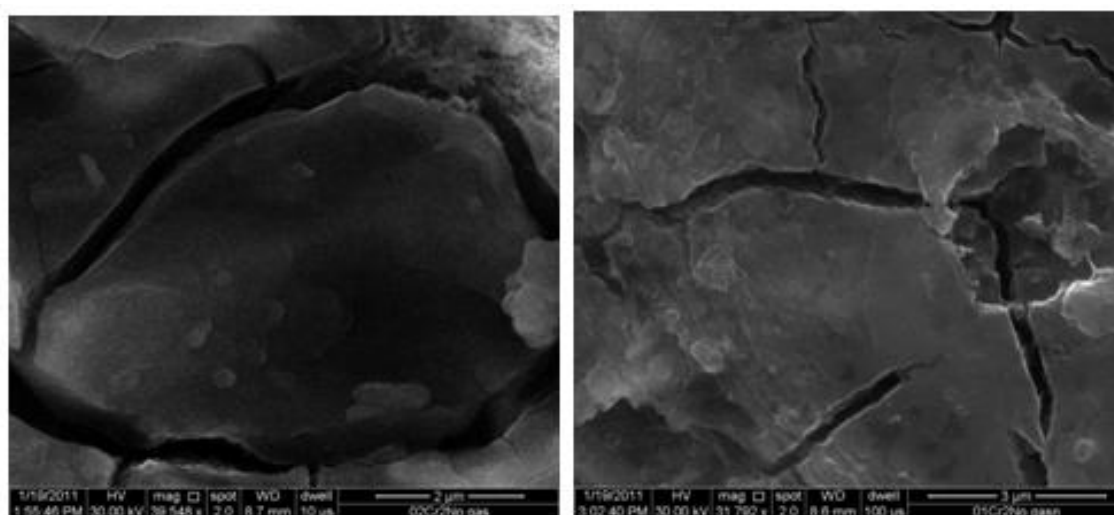


Figure 9. SEM images of anode surface morphology subjected to two different initial potassium dichromate solution concentrations: (a) 0.02 M, (b) 0.01 M, both at no gas flow, 5 mA/cm^2 current density, and 1.5 wt. % NaCl.

Table 2. Anode surface composition after subjected to different initial concentration of potassium dichromate solution at 1.5 wt. % NaCl solution, and no gas flow.

Surface location	Initial potassium dichromate solution concentration			
	0.01M		0.02M	
	%Cr	%Fe	%Cr	%Fe
Overall	2.63	97.37	5.88	94.05
001	6.96	93.04	2.07	97.93
003	1.01	98.99	1.82	98.18

3.3. Electric power consumption

In order to assess the economic viability of the present technique, unit energy consumption per unit volume of waste solution, (Φ) in kW.h/m³, was calculated under different conditions using the following equation [24]:

$$\Phi = EIt/1000 V$$

Where, E is the cell voltage in volt, I is the cell current in ampere, t is the time of electrocoagulation in hour, and V is the solution volume in m³. Figure 10 shows the effect of current density on the unit energy consumption at different air flow rate. Energy consumed per unit volume increases with current density owing to the increase in the cell voltage E which is given by

$$E = E_{eq} + \eta_c + \eta_a + IR$$

Where E_{eq} is the equilibrium cell voltage, η_c and η_a are polarization at the cathode and anode respectively, and IR is the voltage drop due to the cell resistance R. The cell voltage increases with current density as a result of increasing activation polarization at the cathode and anode according to Tafel's equation [25] and the increase in voltage drop due to cell resistance (IR). Figure 10 shows that gas sparging has a much lesser effect on cell energy consumption than current density.

Figure 11 shows the effect of gas sparging on both cell energy consumption and its percentage removal efficiency.

Results show that by changing the gas flow rate from zero to 10 l/min, an approximately 62% increase in Cr(VI) removal can be achieved for only a 12 % increase in cell energy consumption. An overall economic evaluation of the reactor performance measured by the ratio of percent of Cr(VI) removed to cell energy consumption versus sparging gas flow rate at different current densities is shown in figure 12.

Results show that gas sparging has a profound effect on cell economic performance at lower current densities. Higher current density dramatically decreases the cell performance as well as diminishes the effect of gas sparging on its performance. The above results indicate that gas sparging

improves the electrochemical cell productivity per unit energy consumed owing to the decrease in concentration polarization at the anode as a result of the turbulence induced by the gas bubbles.

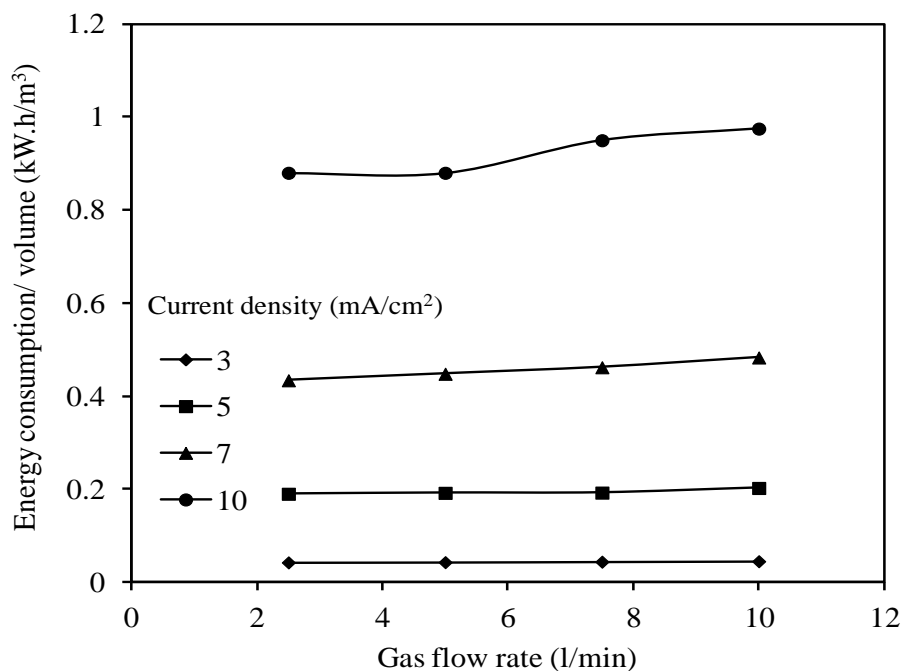


Figure 10. Energy consumption vs. gas flow rate at different current densities, 0.01 M initial potassium dichromate solution concentration, and 1.5 wt.% NaCl concentration

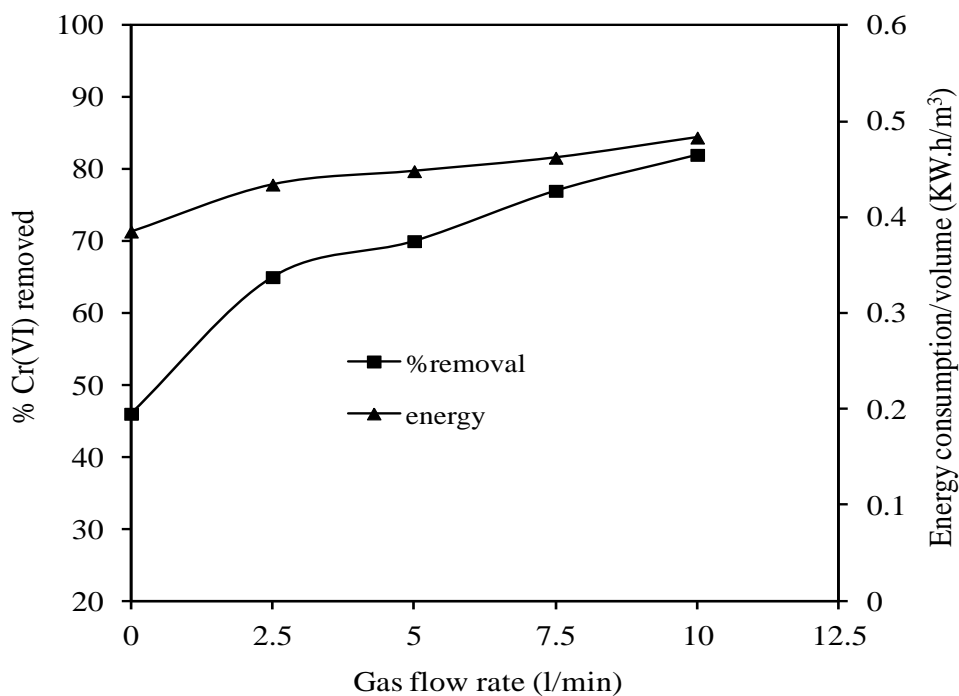


Figure 11. % Cr(VI) removed and energy consumed vs. gas flow rate at 0.01 M initial potassium dichromate solution concentration, and 1.5 wt.% NaCl concentration

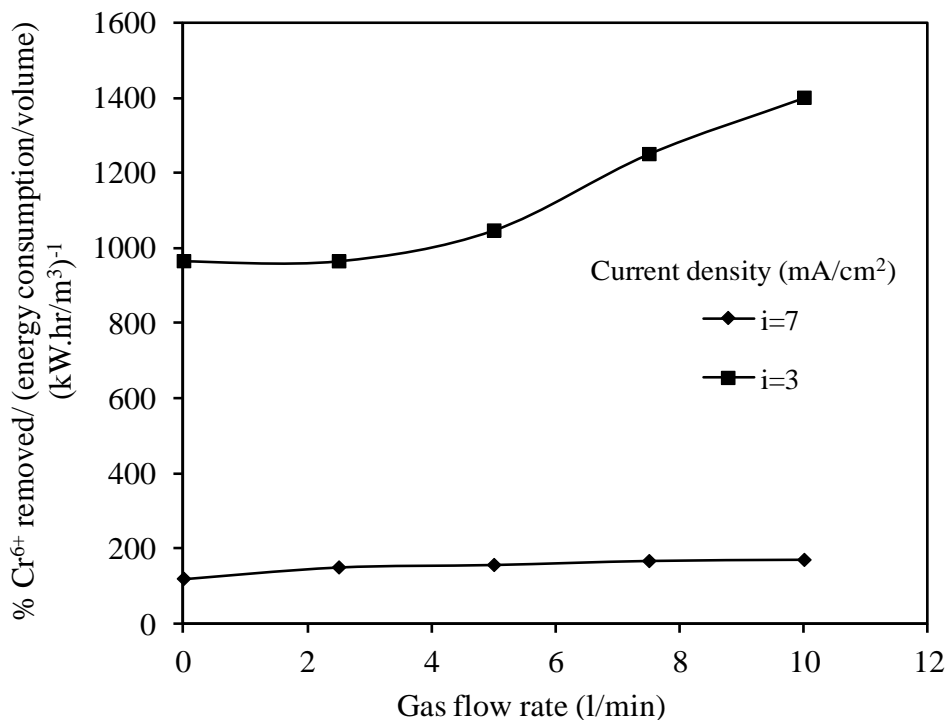


Figure 12. % Cr(VI) removed per energy consumed vs. gas flow rate at two different current densities, .01 M initial potassium dichromate solution concentration, and 1.5 wt.% NaCl concentration

4. CONCLUSIONS

Gas sparging was used in this study to improve the performance of a batch electrocoagulation reactor employing monopolar iron electrodes for Cr(VI) removal. The effect of several variables on the unit performance was investigated. Depending on gas flow rate used, gas sparging was found to improve the productivity of the unit by 40 to 50%. Moreover, Cr(VI) removal increases by increasing both current density and NaCl concentration, while it decreases by increasing the initial Cr(VI) concentrations. The electrode potential, on the other hand, is found to decrease by increasing gas flow rate, while the overall cell voltage increases. An economic analysis on the unit, based on percent of chromium removed per energy consumed, show that, at lower current densities, increasing the gas flow rate profoundly improves the percent of chromium removal per unit energy consumed. However, this effect diminishes at higher current densities at which the reactor economic performance, regardless of the sparging conditions, is drastically decreased. These results clearly show that gas sparging provides a simple, cheap, and practical method to greatly improve the performance of a batch electrocoagulation reactor and its economic viability.

ACKNOWLEDGMENT

This work was funded by the Deanship of Scientific Research of King Abdulaziz University, Jeddah, Saudi Arabia under grant No. (5-135-D1432).

References

1. V.K. Gupta, M. Gupta, S. Sharma, *Water Res.* 35 (5) (2001) 1125-1134.
2. M. Ajmal, R.A.K. Rao, B.A. Siddiqui, *Water Res.* 30 (6) (1996) 1478-1482.
3. C. Namasivayam, R.T. Yamuna, *Chemosphere* 30(1995)561-578.
4. K. Muthukumar, N. Balasubramanian and T.V. Ramakrishna, *Met Finish*, 93 (1995) 11-21
5. Control and Treatment Technology for the Metal Finishing Industry, US, EPA, (1980).
6. Y. Hisamatsu and Y. Kitajima, *J. Metal Finish. Soc. Japan*, 19 (1968) 466-477.
7. F. Sevim and D. Demir, *Chem. Eng. J.* 143 (2008) 161–166.
8. D.W. Blowes, C.J. Ptacek, S.G. Benner, C.W.T. McRae, T.A. Bennett, R.W. Puls, *J. Contam. Hydrol.* 45 (2000) 123–137.
9. N.Kongsricharoen, C.Polprasert, *Water Sci. Technol.* 34(9)(1996)109.
10. I. Heidmann and W. Calmano, *Sep. and Purif. Tech.*, 61(2008)15-21
11. F. Shen, X. Chen, P. Gao and G. Chen, *Chem. Eng. Sci.*, 58(3-6) (2003)987-993.
12. A.H. El-Shazly, A.A. Mubarak and A.H. Konsowa, *Desalination* 85(2005)307 -316.
13. A.H. El-Shazly, *Bulg. Chem. Comm.*, 42(1)(2010)55-61.
14. L. Guang, Y. Xiaogang and D. Gance, *Chem. Eng. Sci.* 64(2009) 5104 – 5116.
15. N. Ibl, R. Kind and E. Adam, *An Quim*, 71(1975)1008-1016.
16. Daous, M., S. Nosier, and K. AlGhamdi, *Chem Eng Res Des* (2011), doi: 10.1016/j.cherd.2011.09.006
17. L. Sigrist, O. Dessenbach and N. Ibl, *J. Appl. Electrochem.* 22(1979) 1393-1403.
18. G.H. Sedahmed, M.S. Abdo, M.A. Kamal, O.A. Fadaly, and H.M. Osman, *Chem. Eng. Proc.*, 40(3)(2001)195-200.
19. S.A. Nosier, A. El-Kayar, H.A. Farag and G.H. Sedahmed, *Int. commun. Heat Mass Transfer*, 24(5) (1997)733-740.
20. M.A. Zarraa, M.Z. El-Abd, Y.A. Eltawil, H.A. Farag and G.H. Sedahmed, *Chem. Eng. J. and Biochem. Eng. J.* 54(1) (1994)51-56.
21. M.M. Zaki, I. Nirdosh and G.H. Sedahmed, *Chem. Eng. Comm.* 186(1) (2001)43-56.
22. A.L. Vogel, A Text-Book of Quantitative Inorganic Analysis, 3rd edition, Longman, London, 1975.
23. M.M Emamjomeh and M. Sivakumar, *J. Environ. Manag.* 90(2009) 1663–1679
24. P. Gao, X. Chen, F. Shen and G. Chen, *Sep. Purif. Tech.* 43(2005)117–123.
25. M.G. Fontana, Corrosion Engineering, 3rd ed., McGraw Hill, 1986.